



Article

Genotoxicity and Cytotoxicity Induced in *Zygophyllum fabago* by Low Pb Doses Depends on the Population's Redox Plasticity

Antonio López-Orenes ¹, Conceição Santos ², Maria Celeste Dias ³ , Helena Oliveira ⁴, María Á. Ferrer ¹ , Antonio A. Calderón ¹ and Sónia Silva ^{5,*}

¹ Department of Agricultural Engineering, Universidad Politécnica de Cartagena, Paseo Alfonso XIII 48, 30203 Cartagena, Spain; antonio.orenes@upct.es (A.L.-O.); manglees.ferrer@upct.es (M.Á.F.); antonio.calderon@upct.es (A.A.C.)

² Department of Biology & LAQV/REQUIMTE, Faculty of Sciences, University of Porto, Campo Alegre, 4169-007 Porto, Portugal; csantos@fc.up.pt

³ Centre for Functional Ecology (CEF), Department of Life Science, University of Coimbra, Calçada Martim de Freitas, 3000-456 Coimbra, Portugal; celeste.dias@uc.pt

⁴ Department of Biology, CESAM, University of Aveiro, Campus Universitário de Santiago, 3810-193 Aveiro, Portugal; holiveira@ua.pt

⁵ Department of Chemistry, LAQV-REQUIMTE, University of Aveiro, 3810-193 Aveiro, Portugal

* Correspondence: soniasilva@ua.pt; Tel.: +351-234-370-766



Citation: López-Orenes, A.; Santos, C.; Dias, M.C.; Oliveira, H.; Ferrer, M.Á.; Calderón, A.A.; Silva, S. Genotoxicity and Cytotoxicity Induced in *Zygophyllum fabago* by Low Pb Doses Depends on the Population's Redox Plasticity. *Horticulturae* **2021**, *7*, 455. <https://doi.org/10.3390/horticulturae7110455>

Academic Editors: Luisa Louro Martins and Miguel Pedro Mourato

Received: 16 September 2021

Accepted: 2 November 2021

Published: 3 November 2021

Publisher's Note: MDPI stays neutral with regard to jurisdictional claims in published maps and institutional affiliations.



Copyright: © 2021 by the authors. Licensee MDPI, Basel, Switzerland. This article is an open access article distributed under the terms and conditions of the Creative Commons Attribution (CC BY) license (<https://creativecommons.org/licenses/by/4.0/>).

Abstract: Lead (Pb) soil contamination remains a major ecological challenge. *Zygophyllum fabago* is a candidate for the Pb phytostabilisation of mining tailings; nevertheless, the cytogenotoxic effects of low doses of Pb on this species are still unknown. Therefore, *Z. fabago* seeds collected from non-mining (NM) and mining (M) areas were exposed to 0, 5 and 20 μ M Pb for four weeks, after which seedling growth, Pb cytogenotoxic effects and redox status were analyzed. The data revealed that Pb did not affect seedling growth in M populations, in contrast to the NM population. Cell cycle progression delay/arrest was detected in both NM and M seedlings, mostly in the roots. DNA damage (DNAd) was induced by Pb, particularly in NM seedlings. In contrast, M populations, which showed a higher Pb content, exhibited lower levels of DNAd and protein oxidation, together with higher levels of antioxidants. Upon Pb exposure, reduced glutathione (GSH) and non-protein thiols were upregulated in shoots and were unaffected/decreased in roots from the NM population, whereas M populations maintained higher levels of flavanols and hydroxycinnamic acids in shoots and triggered GSH in roots and shoots. These differential organ-specific mechanisms seem to be a competitive strategy that allows M populations to overcome Pb toxicity, contrarily to NM, thus stressing the importance of seed provenance in phytostabilisation programs.

Keywords: antioxidant response; cytotoxicity; genotoxicity; Pb tolerance; phytotoxicity

1. Introduction

Lead (Pb) continues to be a major environmental pollutant and health hazard, globally contaminating agricultural soils and water, and entering the food chain [1]. Pb toxicity to plants includes disturbances in nutrient uptake and photosynthesis, ultimately resulting in reduced plant growth [2]. Pb absorption is conditioned by other metals and the competition of nutrients for the same cation transporters, which also assist Pb transport across plasma membranes [3,4]. Cells may use precipitation, chelation and sequestration processes to avoid Pb toxicity [5], and Pb may be immobilized in the root cell wall [6] or, inside the cell, be mobilized and accumulated in the vacuole. Once inside the cell, Pb may interact with proteins and other biomolecules, as well as increase reactive oxygen species (ROS) via indirect processes, including the inhibition of enzymes (as it is a non-redox-active metal), or it may displace essential cations from binding sites, disturbing cell metabolism and function [2,7].

Plant species growing on metal-polluted soils have, in principle, a higher potential to be used in the phytoremediation programs of metal-contaminated environments since they are often genetically better equipped to survive and reproduce under metal-polluted environments [8]. Furthermore, these species are suitable models to study the mechanisms underlying the tolerance to metals [9,10]. The Syrian beancaper (*Zygophyllum fabago* L.) is a perennial shrub able to grow in nutrient-poor soils, as well as in areas severely contaminated with heavy metals [8,11,12]. Previous studies showed that *Z. fabago* populations, both adapted and non-adapted to metals, responded differently to high doses of Pb (the detected toxicity was 25 μM), with the adapted plants altering their antioxidative metabolisms more promptly and efficiently [13–15]. Showing a constitutively higher and more efficient reactive oxygen species (ROS)-processing capability in *Z. fabago* populations adapted to Pb, it is unclear if Pb induces genotoxicity and cell cycle disorders in the different populations. For other sensitive species, it was proposed that the Pb-generated ROS may play a role in genotoxic effects, which may include chromosomal aberration, micronuclei formation and DNA degradation [4,16–18]. However, this genotoxicity depends on the species, dose, exposure and selected endpoints. Most of the Pb phytotoxicity studies use Pb levels ranging from the micromolar to millimolar [19], which are higher than the nanomolar doses found in non-contaminated soil solutions, or the micromolar levels reported for soil solution in contaminated areas [20]. Nevertheless, the Pb concentration in topsoils may reach 20 mg Kg^{-1} in non-contaminated areas [20]. In order to trigger Pb toxicity, Silva et al. [18] found that doses below the Pb maximum admissible for irrigation waters (5 mg L^{-1}) [21] induced genotoxicity in lettuce plants.

Aligned with these findings, we aim to understand if the chronic exposure of *Z. fabago*, a species that spontaneously colonizes mining areas, to realistic Pb doses ranging from 5 μM to 20 μM $\text{Pb}(\text{NO}_3)_2$ (corresponding to $\sim 1 \text{ mg L}^{-1}$ and $\sim 4 \text{ mg L}^{-1}$ Pb), induces cytogenotoxic effects in the roots and shoots of *Z. fabago* plants. Additionally, we aim to understand how these putative effects depend on the origin of the seed populations (NM population seeds collected in non-mining soils vs. M population seeds collected in mining soils), which differ in their constitutive redox statuses.

2. Materials and Methods

2.1. Plant Material, Culture and Exposure to Pb

Two populations of *Z. fabago* from mining sites (M) (Agustin and Mercader), and one population 1 km away from M, a non-mining impacted area (NM), were used to conduct the experiments [22]. Seeds from each population were collected at Cartagena-La Unión Mining District (southeast Spain). The soils of these mining sites are characterized by high concentrations of heavy metals, in particular Pb [22]. The total Pb concentrations in the rhizosphere mine soils were within the range 2685–3439 $\mu\text{g g}^{-1}$, whereas the levels in the rhizosphere of non-mining soils were $< 650 \mu\text{g g}^{-1}$ [22].

Fifty seeds were germinated and grown in perlite culture in plastic trays (2 L), irrigated with 500 mL of $\frac{1}{4}$ Hoagland's No. 2 Basal Salt Mixture, and supplemented once with 0, 5 or 20 μM $\text{Pb}(\text{NO}_3)_2$ (pH 5.0). Under these conditions, 100% of Pb solubility was assured in the nutrient solution, according to the Visual MINTEQ version 3.1 chemical equilibrium modelling program (<http://vminteq.lwr.kth.se/> (last accessed on 23 July 2021)).

The seedlings growth took place in a greenhouse under controlled conditions of temperature ($25/20 \pm 2 \text{ }^\circ\text{C}$), photoperiod (day/night, 16 h/8 h), and light provided by lamps Philips SON-T Greenpower, HPS 600 W (photosynthetic active radiation (PAR) at the plant level was $470 \mu\text{mol m}^{-2} \text{ s}^{-1}$).

After four weeks of growth, roots were washed in 5 mM CaCl_2 , rinsed in distilled water and blotted with filter paper. Then, seedling root and shoot length, fresh and dry mass (determined in oven-dried samples after one week at $80 \text{ }^\circ\text{C}$) as well as leaf relative water content (RWC) were determined using five seedlings per treatment and per population.

The rest of the seedlings were randomly divided into four groups (8–9 seedlings per treatment and populations were pooled together and considered as one replicate), separated

into shoots and roots, and immediately flash frozen in liquid nitrogen, cryogenically pulverized using an analytical mill, and stored at $-80\text{ }^{\circ}\text{C}$ for further biochemical analysis. Thus, for each biochemical assay, four biological replicates, each one from 8–9 seedlings, and two technical replicates per sample were performed.

2.2. Photosynthetic Pigment Quantification

The extraction and analysis of photosynthetic pigments was carried out as previously described [14,15]. In short, liquid nitrogen-powdered shoot samples (~0.1 g) were extracted with 100% methanol (1.2 mL) using sonication at $40\text{ }^{\circ}\text{C}$ for 30 min. After centrifugation ($15,000\times g$ for 15 min at $4\text{ }^{\circ}\text{C}$), the absorbance of the supernatants was read at 666, 653 and 470 nm in a 96-well plate reader (Multiskan GO, Thermo Scientific, Waltham, MA, USA) to calculate the content of chlorophyll *a* (Chl *a*) and *b* (Chl *b*) and total carotenoids (xanthophylls and carotenes).

2.3. Pb Quantification in Tissues

Dried samples of shoots and roots were incinerated at $450\text{ }^{\circ}\text{C}$ (8 h) and ashes digested in nitric acid 70%. Pb content was quantified by inductively coupled plasma mass spectrometry (ICP-MS, Agilent 7500A, Santa Clara, CA, USA). The Pb root-to-shoot transfer coefficient (TC) was given by $\text{TC} = [\text{Pb}]_{\text{shoot}}/[\text{Pb}]_{\text{root}}$. Six plants per treatment and population were used.

2.4. DNA Fragmentation

The DNA fragmentation and associated disorders were assessed using the comet assay, as described by Gichner et al. [23], with the slight modifications by Rodriguez et al. [24]. Briefly, leaf and root samples were sliced in cold 0.4 M Tris buffer (pH 7.5). The nuclei suspension and 1% low-melting-point agarose were spread on a slide covered with 1% normal-melting-point agarose layer. Slides were immersed in alkaline buffer (0.30 M NaOH, 1 mM EDTA, pH > 13) for 15 min prior to electrophoresis (0.74 V cm^{-1} and 300 mA for 25 min), followed by neutralization with 0.4 M Tris buffer (pH 7.5). Then, slides were analysed under a fluorescence microscope (Nikon Eclipse 80i, Düsseldorf, Germany) after staining with ethidium bromide. The comets were classified by visual scoring from class 0 (minimal DNA damage) to class 4 (maximum DNA damage). DNA damage was calculated as $\text{DNA}_{\text{d}} = (\% \text{ cells in class } 0 \times 0) + (\% \text{ cells in class } 1 \times 1) + (\% \text{ cells in class } 2 \times 2) + (\% \text{ cells in class } 3 \times 3) + (\% \text{ cells in class } 4 \times 4)$. More than 300 nucleoids were scored for each treatment and 3 replicates were used.

2.5. Flow Cytometric Analysis

The DNA content of the two M and the NM populations was determined against the internal standard *Pisum sativum* cultivar 'Ctirad' ($2\text{C} = 9.09\text{ pg DNA}$, provided by J. Dolezel, Institute of Experimental Botany, Olomouc, Czech). Leaf DNA content and cell cycle progression disturbances in leaf and root samples were compared by flow cytometry (FCM) [24,25]. Leaves and roots were chopped in Woody Plant Buffer [26] and nuclei were stained with propidium iodide (PI). Around 2000–4000 nuclei/samples were analysed in a flow cytometer (EPICS-XL Coulter, Brea, CA, USA) at 488 nm equipped with an Argon laser (15 mW, 488 nm). Results were acquired using the SYSTEM II software (v. 3.0, Beckman Coulter, Brea, CA, USA) and side scatter, forward scatter, and cell cycle distributions were determined according to our standard protocols [25]. For FCM analysis, 6 replicates for each treatment were used.

2.6. Quantification of Total Antioxidant Activity and Phenolic Compounds

The analysis of the total antioxidant activity (TAC) was performed according to Pérez-Tortosa et al. [27] using both shoot and root methanolic extracts obtained as mentioned above. Briefly, 20 μL of methanolic extracts were used to determine their ability to scavenge for the radicals DPPH• (2,2-diphenyl-1-picrylhydrazyl), and ABTS•+ [2,2'-azino-bis(3-

ethylbenzothiazoline-6-sulphonate)], and to reduce Fe(III) to Fe(II) using the ferric-reducing antioxidant power (FRAP) assay.

The methanolic extracts (10–20 μL) were also used to determine the concentration of total soluble phenolic compounds (TPC), flavonoids, flavanols and hydroxycinnamic acids (HCAs) as described by López-Orenes et al. [14,15]. In short, TPC was assessed by the Folin–Ciocalteu method using gallic acid (range 50 to 3000 μM) as standard. The total flavonoid content was determined by the aluminum chloride assay with rutin (range 50 to 2000 μM) as standard. Total flavanols were determined with DMACA (*p*-dimethylaminocinnamaldehyde) reagent and (+)-catechin (range 10 to 500 μM) as a reference, and HCAs were measured using Arnov's reagent and caffeic acid (range 50 to 3000 μM) as standard.

The lignin was determined on pellets from methanolic extractions by the thioglycolic acid precipitation method using a linear calibration curve (range 0.02–0.12 mg/mL) performed with commercial alkali lignin [14].

2.7. Determination of Ascorbate, Dehydroascorbate, Glutathione and Total Soluble Non-Protein Thiols

For ascorbate (AsA) and dehydroascorbate (DHA), ~0.1 g of liquid nitrogen-powdered shoot or root samples were extracted with 1.2 mL of 6% trichloroacetic acid (TCA). The homogenates were spun ($13,000 \times g$ for 5 min at 4 °C), and the supernatants were used for the analysis of AsA using the α - α' -bipyridyl-based spectrophotometric assay [14,15].

The reduced glutathione (GSH) levels were determined fluorimetrically using an *o*-phthalaldehyde (OPA) probe as previously described [28]. Liquid nitrogen-powdered samples (~0.1 g) were extracted with 1.2 mL of 20 mM HCl, 5 mM EDTA (ethylenediaminetetraacetic acid) and 5% TCA. After centrifugation ($15,000 \times g$ for 20 min at 4 °C), the supernatants were used for the analysis. OPA-derived fluorescence was measured at 365 nm excitation and 430 nm emission using a NanoDrop™ 3300 spectrofluorimeter.

The total soluble non-protein thiols (NPT) were determined from frozen samples (~0.1 g) extracted in 1.2 mL of 0.2 N HCl and 6% (*w/v*) polyvinylpyrrolidone (PVPP), and quantified using DTNB [5,5'-dithio-(2-nitrobenzoic acid)] according to [29]. Total phytochelatin (PCs) levels were estimated from the difference between NPT and GSH [30].

2.8. Determination of Hydrogen Peroxide, Lipid Peroxidation and Protein Oxidation

Hydrogen peroxide levels were determined by the ferrous ion oxidation–xylenol orange (FOX) method as previously described [14]. Briefly, ~0.1 g of liquid nitrogen-powdered samples were homogenized in 1.2 mL of 0.2 N HCl and 6% (*w/v*) polyvinylpyrrolidone (PVPP). After centrifugation ($12,000 \times g$ for 10 min at 4 °C), 50 μL of the supernatants were mixed with 200 μL of the assay solution (250 μM ferrous sulfate ammonium, 100 μM sorbitol, 100 μM xylenol orange, 25 mM sulfuric acid and 1% *v/v* ethanol). After 45 min incubation in the dark, at room temperature, the absorbance at 560 nm of the Fe^{3+} xylenol orange complex formed was measured in a 96-well plate reader (Multiskan GO, Thermo Scientific, Waltham, MA, USA).

The lipid peroxidation was determined following the malondialdehyde (MDA) formation using the thiobarbituric acid reactive method [31]. In short, frozen samples (~0.1 g) were homogenized with 1.2 mL of 0.1% TCA (*w/v*). After centrifugation ($10,000 \times g$, 10 min at 4 °C), two aliquots (200 μL) of each supernatant were taken. One aliquot was mixed with 200 μL of 20% (*w/v*) TCA and 0.01% (*w/v*) butylated hydroxytoluene; the other was mixed with 200 μL of 20% (*w/v*) TCA, 0.01% (*w/v*) butylated hydroxytoluene and 0.5% (*w/v*) thiobarbituric acid (TCA + TBA). After incubation at 95 °C for 30 min, the tubes were cooled and centrifuged ($12,000 \times g$, 5 min, and 4 °C). The specific absorbance was measured at 532 nm and the non-specific absorbance at 600 nm. The level of MDA was determined by subtracting the non-specific absorbance from the specific absorbance and using the extinction coefficient of $155 \text{ mM}^{-1} \text{ cm}^{-1}$.

Protein oxidation was assayed by reacting protein carbonyl groups with 2,4-dinitrophenylhydrazine [31]. Briefly, frozen samples (~0.25 g) were homogenized in 1 mL of ice-

cold buffer (0.1 M potassium phosphate, pH 7.0) supplemented with 0.1% (*w/v*) protease inhibitor mix (complete protease inhibitor cocktail, Roche, Mannheim, Germany) and 0.05% (*w/v*) cysteine. After centrifugation ($15,000\times g$, 15 min, and 4 °C), two aliquots (200 μL) of each supernatant were taken. One aliquot was incubated with 20 mM 2,4-dinitrophenylhydrazine (DNPH) in 2 M HCl (1:2, *v/v*), which reacted with carbonyl groups. The other aliquot was incubated with HCl without DNPH and was used as a blank for each sample. After 1 h of incubation at room temperature carbonyl proteins were precipitated with 20% (*w/v*) TCA and rinsed with ethanol:ethylacetate (1:1, *v/v*) three times. Then, the pellets were resuspended in 6 M guanidine hydrochloride and absorbance was read at 360 nm (extinction coefficient of $22,000\text{ M}^{-1}\text{ cm}^{-1}$).

The protein concentrations were measured by the Bradford method, using bovine serum albumin (BSA) as the standard.

2.9. Statistical Analysis

Significance of differences ($p < 0.05$) between groups was tested using one-way analysis of variance (ANOVA), combined with Tukey's honestly significant difference (HSD) post hoc test, using the SPSS software (version 19.0; SPSS Inc., Chicago, IL, USA). Principal component analysis (PCA) was performed using the "CANOCO for Windows" program v4.02.

3. Results

3.1. Comparative Effects of Low Pb Doses on Germination, Seedling Growth and Photosynthetic Pigments

The germination rate decreased in both Pb doses in non-mining seedlings, whereas, in Agustín, decreased only at 20 μM Pb; in Mercader it was not affected (Table S1). In the absence of Pb, seeds from the M populations showed different performances according to the regions of provenance, with those from Mercader showing an initial delay in germination but later reaching the values of the NM seeds (>75%) at day 18 (Table S1). Pb drastically decreased the germination rate in the NM population (54%), whereas, in both M populations, germination was not significantly affected (Table S1).

The growth of non-mining seedlings (biomass and length) was severely compromised by Pb even at the lowest level, while M populations were not significantly affected, particularly Mercader (Figure 1, Table S1).

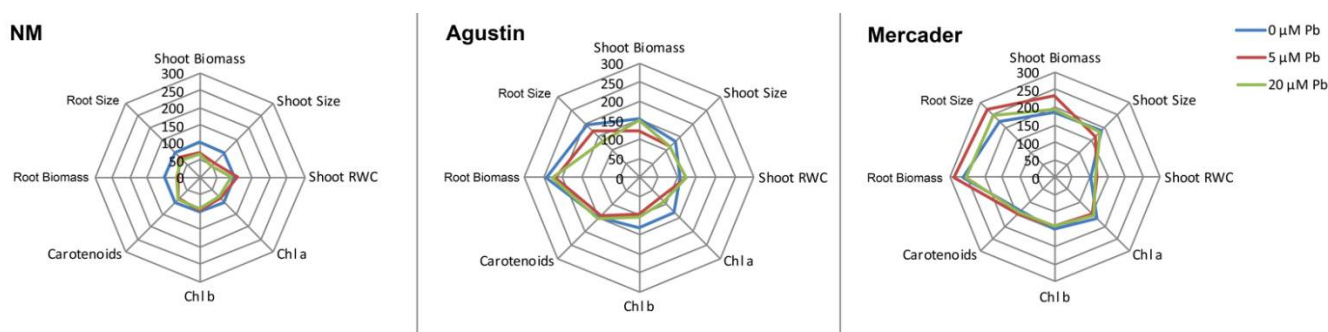


Figure 1. Radar chart of the effects of Pb treatments [0, 5 and 20 μM $\text{Pb}(\text{NO}_3)_2$] for 4 weeks on growth parameters (shoot and root biomass, shoot and root size), RWC and photosynthetic pigment levels of seedlings from non-mining (NM) and mining (Agustín and Mercader) *Z. fabago* populations exposed to 0, 5 and 20 μM $\text{Pb}(\text{NO}_3)_2$ for 4 weeks. Parameters values of M populations are expressed as percentage of the corresponding non Pb-treated NM value.

Concerning the pigments, a decrease was detected in Chl *a* and Chl *b* contents in all populations under both Pb doses. Nevertheless, Pb-treated NM seedlings showed a more significant decrease with respect to the control [Chl *a* (−22%), Chl *b* (−9%)]. In addition, carotenoids levels were only negatively affected by Pb exposure in NM. On the other hand, M showed higher constitutive levels of carotenoids (~1.3–1.5-fold higher) (Figure 1,

Table S1). After treatment, the relative water content (RWC) increased only in the Pb-exposed shoots of M seedlings (Figure 1, Table S1).

3.2. Pb Content in Shoots and Roots

As expected, the amount of Pb accumulated in shoots and roots significantly increased with the increase in the external Pb concentration in all populations (Figure 2, Table S1). Most of the Pb was accumulated in roots, and only a fraction was translocated to the shoots (Figure 2, Table S1). In absolute terms, the highest levels of Pb were observed in Mercader roots (~4-fold higher than in NM and 1.4-fold higher than in Agustin).

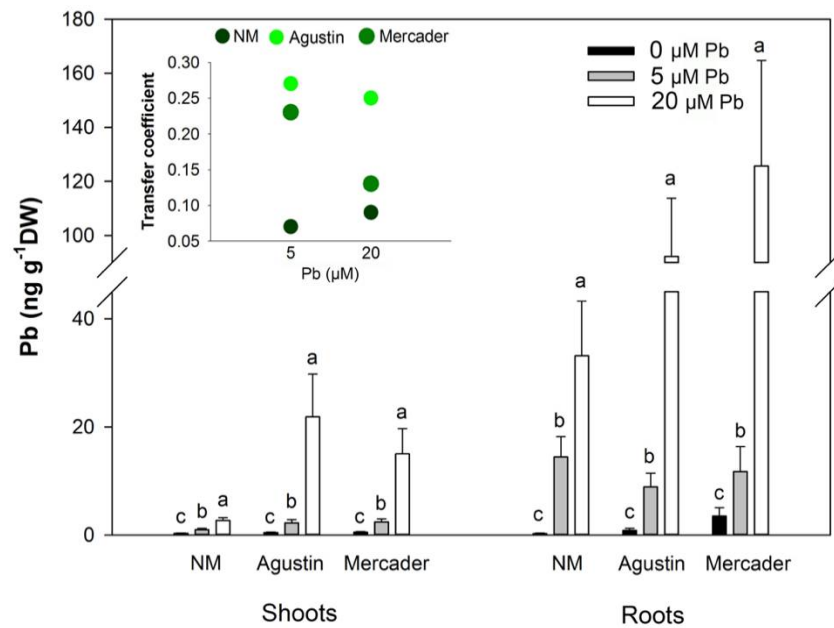


Figure 2. Pb content in roots and shoots and Pb transfer coefficient of NM and M (Agustin and Mercader) *Z. fabago* seedlings exposed to 0, 5 and 20 μM $\text{Pb}(\text{NO}_3)_2$ for 4 weeks. Values are given as mean \pm SE. Different letters correspond to significant differences between Pb doses within the same population and organ.

The root-to-shoot transfer coefficient of Pb was higher in both M populations (>3-fold) than in the NM population (Figure 2, Table S1). On the other hand, the transfer coefficient decreased with the increase in Pb concentration in M populations, contrary to what was observed in NM.

3.3. Genotoxic Effects Induced by Low Pb Doses

Pb induced genotoxicity in all populations and in both leaves and roots (Figure 3A,B). A dose-dependent genotoxic response was clearly observed in Pb-treated, non-mining seedlings, whereas no significant differences between the two doses of Pb were found in M populations, though DNAd levels were always significantly higher in Agustin than in Mercader in the case of both organs.

3.4. Cell Cycle Modulation by Low Doses of Pb

In order to analyze the extent to which Pb treatments affected cell cycle dynamics, we first examined the cell cycle distribution among the three *Z. fabago* populations using Pb-untreated (control) seedlings. As can be observed in Figure 4A, the leaves from the three *Z. fabago* populations showed two clear peaks, I and II, which corresponded to the G_0/G_1 and G_2/M phases, respectively. The high proportion of cells in the G_2/M phase and the presence of a small peak (peak III), in which the PI-fluorescence intensity doubled the value of peak II, suggest the presence of two subpopulations of nuclei which differ in DNA content, i.e., a diploid (A) and a tetraploid (B) subpopulation of nuclei. Thus,

peak I corresponds to the G_0/G_1 phase of the nuclei of the subpopulation A, peak II includes the G_2/M phase of the subpopulation A and the G_0/G_1 phase of the nuclei of the subpopulation B, and peak III corresponds to the G_2/M phase of the subpopulation B.

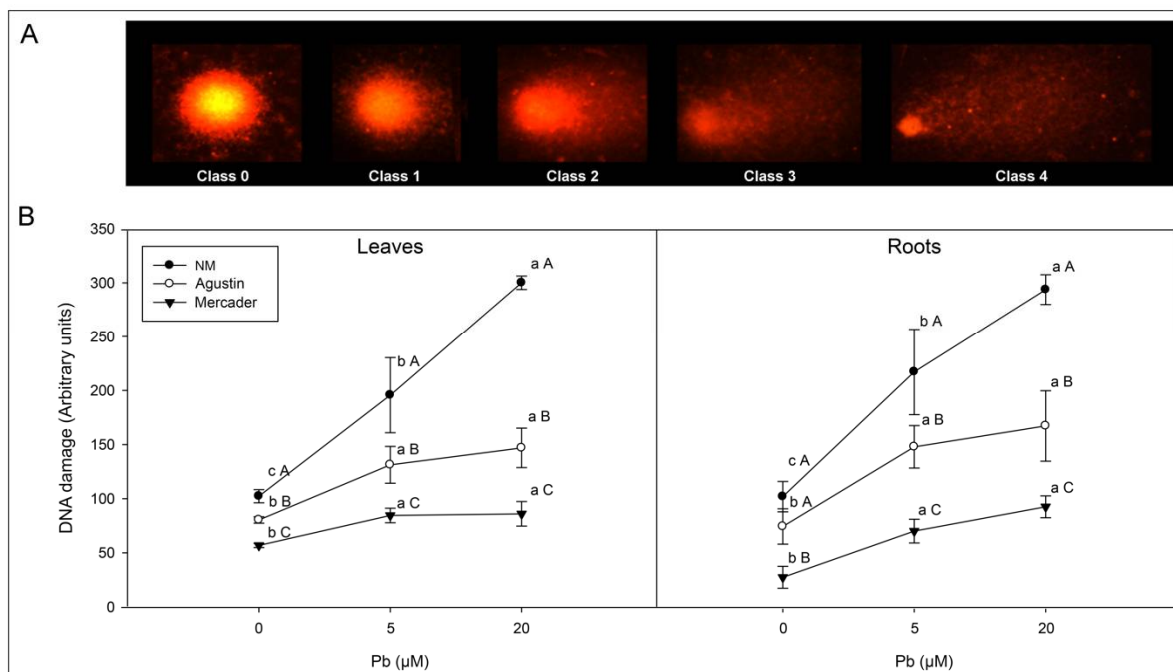


Figure 3. Levels of DNA fragmentation visualized by comet assay in *Z. fabago* exposed to Pb (A). DNA damage (B) in leaves and roots of *Z. fabago* seedlings from non-mining (NM) and mining areas (Agustín and Mercader) exposed to 5 and 20 μM $\text{Pb}(\text{NO}_3)_2$ during 4 weeks. Values are given as mean \pm SE. For each class, different lowercase and uppercase letters mean significant differences between Pb treatments (within the same population) and populations (within the same Pb dose) ($p < 0.05$), respectively.

Concerning genome size, a discrete increase in peak II (<2%) was only detected in Mercader seedlings (Figure 4B).

Some variation was also found between the percentage of nuclei in each peak, as a function of the population origin and the exposure to Pb (Figure 4C,D, Table S2). In the absence of Pb, the differences among the populations were found only in leaves. Both M populations showed a higher percentage of nuclei in peak I than the NM population, whereas in peak II a higher amount was found in NM.

Under Pb exposure, the leaf cell cycle dynamics were not affected in the Agustín population, but an increase in the number of cells in peak I, together with a decrease in peak II, was observed in the Mercader population exposed to 5 μM Pb (Figure 4, Table S2). A similar response was observed in the NM population upon both Pb doses. In roots, the cell cycle dynamics seemed to be less susceptible, as Pb had cytostatic effects only in Agustín at 20 μM Pb, with an increase in the percentage of cells in peak I at the expense of cells in peak II.

3.5. Redox Status Modulation by Low Doses of Pb

It was also determined whether Pb exposure induced the oxidative modifications of proteins and lipids and affected the concentration of H_2O_2 (Figure 5 and Tables S3 and S4). Pb exposure provoked a significant increase in the levels of protein oxidation (measured as protein carbonyl groups) in all *Z. fabago* populations, particularly in NM seedlings, and in both shoots and roots (Figure 5A). A slight increase in the levels of the peroxidation of membrane lipids as a consequence of Pb exposure was also observed in Agustín shoots and in NM roots (Tables S3 and S4).

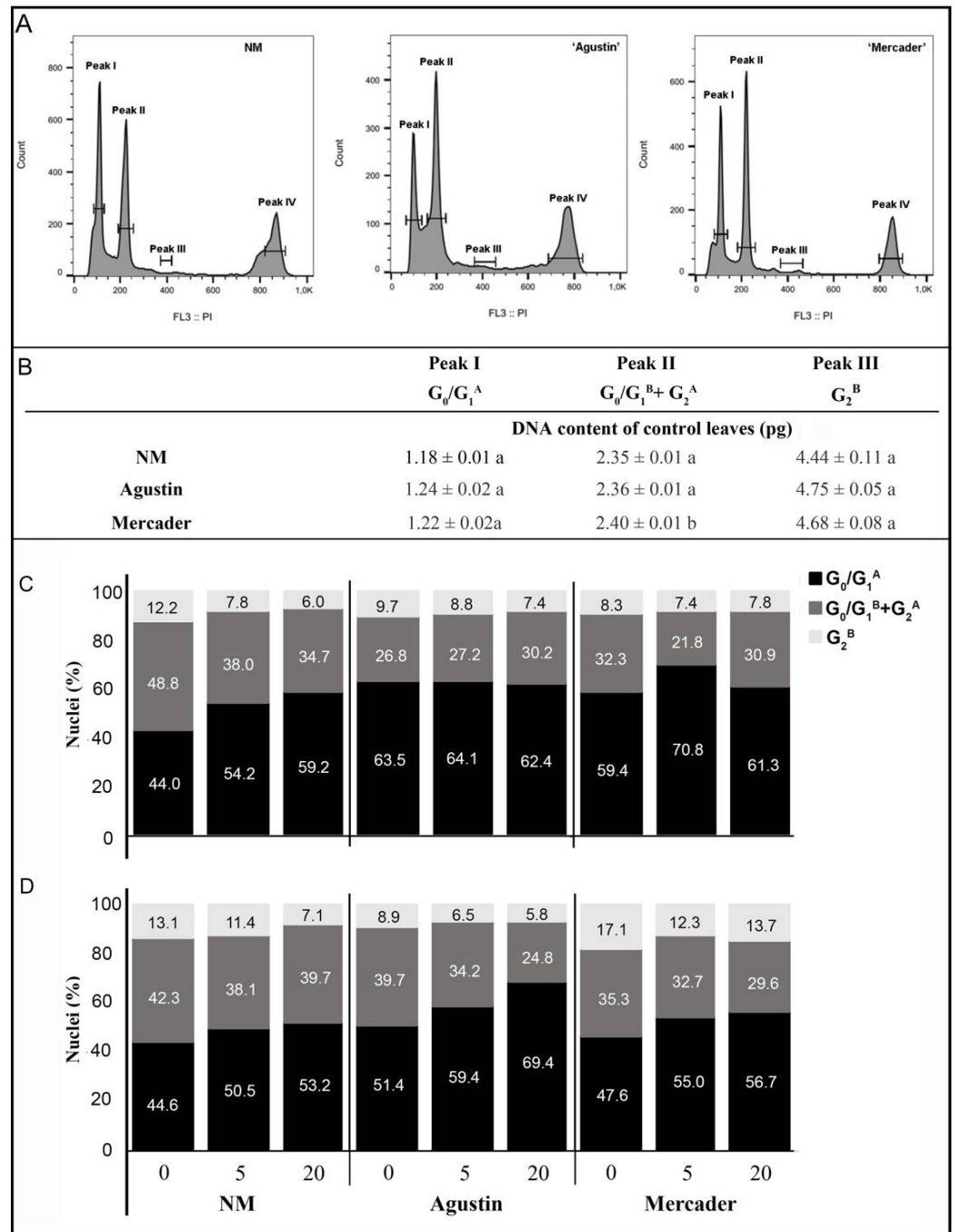


Figure 4. Representative FCM histograms (A), DNA content (pg) (B) from control leaves and percentage of nuclei on each FCM peak in leaves (C) and roots (D) of seedlings from non-mining (NM) and mining areas (Agustin and Mercader); *Z. fabago* populations exposed to 0, 5 and 20 μM $Pb(NO_3)_2$ for 4 weeks. peak I: G_0/G_1 phase of the subpopulation A; peak II: G_1 phase of subpopulation B plus G_2 phase of subpopulation A; peak III: G_2 phase of the subpopulation B. Values are calculated using the G_0/G_1 of the standard *Pisum sativum* (peak IV). Values are given as mean \pm SE. Different letters mean significant differences between populations among the same peak ($p < 0.05$). See Table S2 for statistical analysis results of Figure 4C,D.

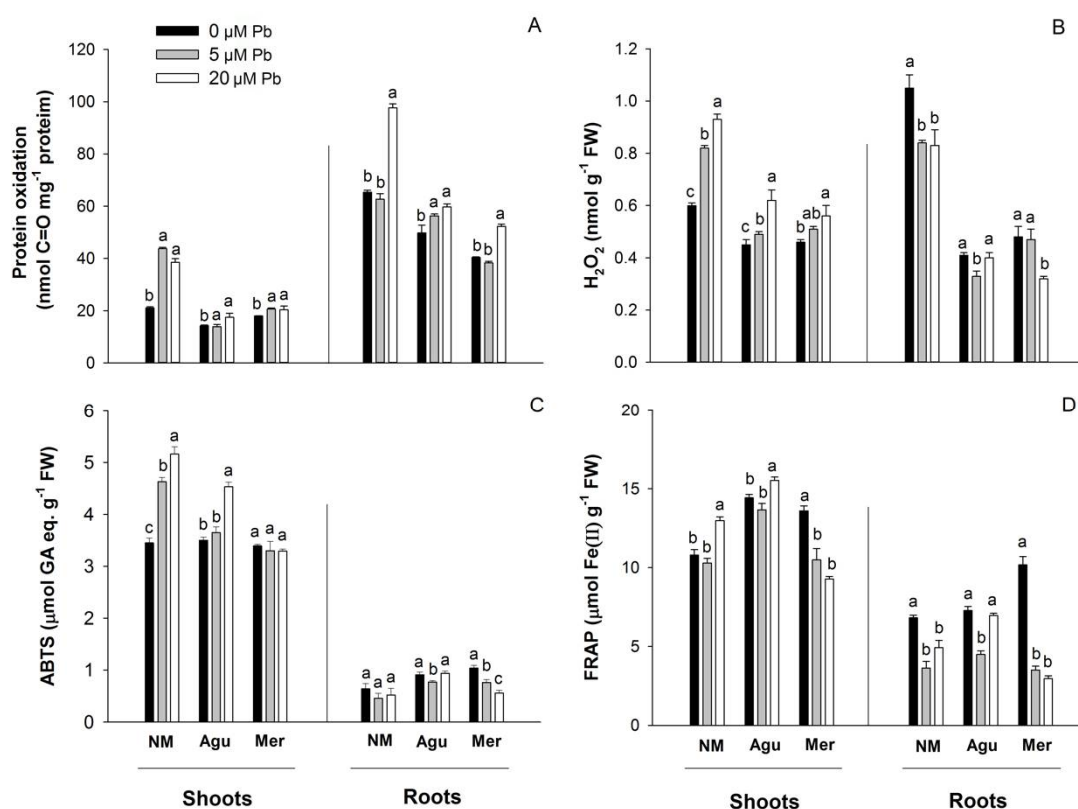


Figure 5. Carbonyl group contents (A), H₂O₂ concentration (B), ABTS radical scavenging capacity (C) and ferric-reducing antioxidant power (D) in shoots and roots of non-mining (NM) and mining Agustin (Agu) and Mercader (Mer) *Z. fabago* seedlings exposed to 0, 5 and 20 μM Pb(NO₃)₂ for 4 weeks. Values are given as mean ± SE. Different letters correspond to significant differences between doses within the same population and organ ($p < 0.05$).

In the absence of Pb, NM seedlings exhibited higher constitutive H₂O₂ levels, particularly in root tissues (1.05 vs. 0.60 μmol g⁻¹ FW), whereas the concentration of H₂O₂ was similar in both organs (~0.45 μmol g⁻¹ FW) in M populations. Pb exposure provoked an increase in the accumulation of H₂O₂ in the shoots of all populations, though this was more marked in NM, whereas in roots the levels of H₂O₂ tended to decrease (Figure 5, Tables S3 and S4).

The total antioxidant capacity (TAC) was also tested through the ABTS, DPPH (Tables S3 and S4) and FRAP methods (Figure 5, Tables S3 and S4). Generally, in the absence of Pb, M seedlings showed a higher TAC than NM seedlings; these values were higher in shoots than in roots (Figure 5, Tables S3 and S4). Pb exposure induced a slight increase, mostly under 20 μM Pb, in the ABTS and FRAP values of NM and Agustin shoots, contrary to those values found in roots (Figure 5). In Mercader seedlings, significant decreases in FRAP were observed in both organs, whereas ABTS and DPPH values were reduced only in roots.

3.5.1. Ascorbate and Thiols

The analyses of the main redox buffers in plant cells, AsA and GSH, as well as non-protein thiols (NPT) are summarized in Figure 6 and Tables S3 and S4. Generally, in the absence of Pb, the levels of the total and reduced AsA were higher in shoots of M, whereas their levels were lower in the roots of Agustin seedlings. Upon Pb exposure, the levels of AsA in shoots remained unchanged in NM and Agustin but dropped to 75% in Mercader at the highest dose of Pb (20 μM). However, in roots, AsA levels tended to increase in Agustin (by 60% in the presence of 20 μM Pb), but decreased in NM and Mercader (by 26% and 48%, respectively). No significant difference in the levels of GSH was found in the absence of Pb among the populations. Pb treatment increased the GSH levels in all populations.

It is worth noticing the increase in GSH only in the shoots of NM seedlings exposed to Pb, whereas a dose-dependent increase in GSH levels was observed in both shoots and roots in M populations. The constitutive levels of NPT in the roots of NM were more than twofold higher than those in the M populations. Upon Pb exposure, NPT content markedly increased in NM (68%) and less in Agustín (31%) shoots, whereas in Mercader remained unchanged. In roots, the NPT levels decreased in both NM and Mercader populations (18% and 28%, respectively). PCs contents in control roots were higher in the NM population, whereas in shoots were similar among all the populations. Interestingly, the Pb exposure substantially increased PCs in the shoots of NM seedlings in a dose-dependent manner (44% and 67% under Pb treatments of 5 and 20 μM , respectively), and in Agustín at the highest Pb dose. On the contrary, in Mercader, the PCs levels decreased. A decreasing trend was observed in the roots and PCs levels in all populations; nevertheless, NM maintained higher levels of PCs than those of M populations.

3.5.2. Phenolic Compounds

The total soluble phenolics (TPC) and HCAs levels were higher in shoots than in the roots in the three populations under both control and Pb conditions (Figure 6, Tables S3 and S4). Nevertheless, the variation in the concentrations of these phenolic compounds in response to Pb was dependent on the population. Thus, TPC increased with the increasing Pb doses in shoots and roots in NM (40% and 20%, respectively) and Agustín (33% and 32%, respectively), but decreased in Mercader, particularly in roots (26% at 20 μM Pb). Contrarily, HCAs decreased in both organs of NM and Agustín, whereas, in Mercader, only decreased in roots. Concerning the flavonoid and flavanol contents in shoots, in the absence of Pb, flavonoid levels were similar among the populations, whereas flavanols contents were higher in M seedlings (~1.5-fold higher than in NM). Upon Pb treatment, a decrease was observed in the flavonoids of all the populations, while the flavanols decreased only in NM (82%) and Agustín (54%) under both Pb treatments, remaining unchanged in Mercader. Overall, the flavanol levels in Mercader under 20 μM Pb were ~9.4-fold higher than in NM. The lignin contents (Tables S3 and S4) in control shoots were higher in NM than in M, whereas similar values were found in the roots of all populations. Under Pb, lignin levels remained unchanged in all populations and in both organs.

3.6. General Overview of *Z. fabago* Response to Pb

In order to have a general overview of the Pb response in both roots and shoots in the three populations, a principal component analysis (PCA) was carried out. In shoots (Figure 7), the PC1, accounting for 47.7% of the variance, was mostly conditioned by DNAd, NPT, H_2O_2 , ABTS, and GSH on the positive side of the axis and by flavanols, biomass, size and chlorophylls on the negative side. PC2, accounting for 14.0%, had strong positive loadings on FRAP, AsA and DHA. In the absence of Pb, the main differences between the M populations and NM population were associated with antioxidants (carotenoids, HCAs, and flavanols), biomass and size. Conversely, the shoots from Pb-treated NM seedlings were closely associated with oxidative markers (DNAd, and protein carbonyl concentrations), H_2O_2 and NPT. In turn, the shoots from Pb-treated M seedlings were divergent in their responses to Pb; Agustín was associated with FRAP, DHA and AsA, while Mercader was associated with chlorophylls.

In roots (Figure 7), the PC1, accounting for 38.8% of the variance, was mostly conditioned by oxidative markers (DNAd, MDA, and protein carbonyl concentrations), H_2O_2 , TPC, DPPH and DHA on the positive side of the axis and by biomass and size on the negative side. PC2, accounting for 16.2%, was defined by FRAP, ABTS and AsA on the positive side of the axis and by GSH on the negative side. The PC1 separated NM and M populations, while the PC2 separated both M controls from Pb-exposed M seedlings. Furthermore, PCA also revealed that Agustín populations showed an intermediate response between those of NM and Mercader. Thus, the response to Pb in roots from NM was associated with oxidative markers (DNAd, carbonyls, and MDA), H_2O_2 , DHA and NPT, whereas, in Mercader, it was associated with size and GSH.

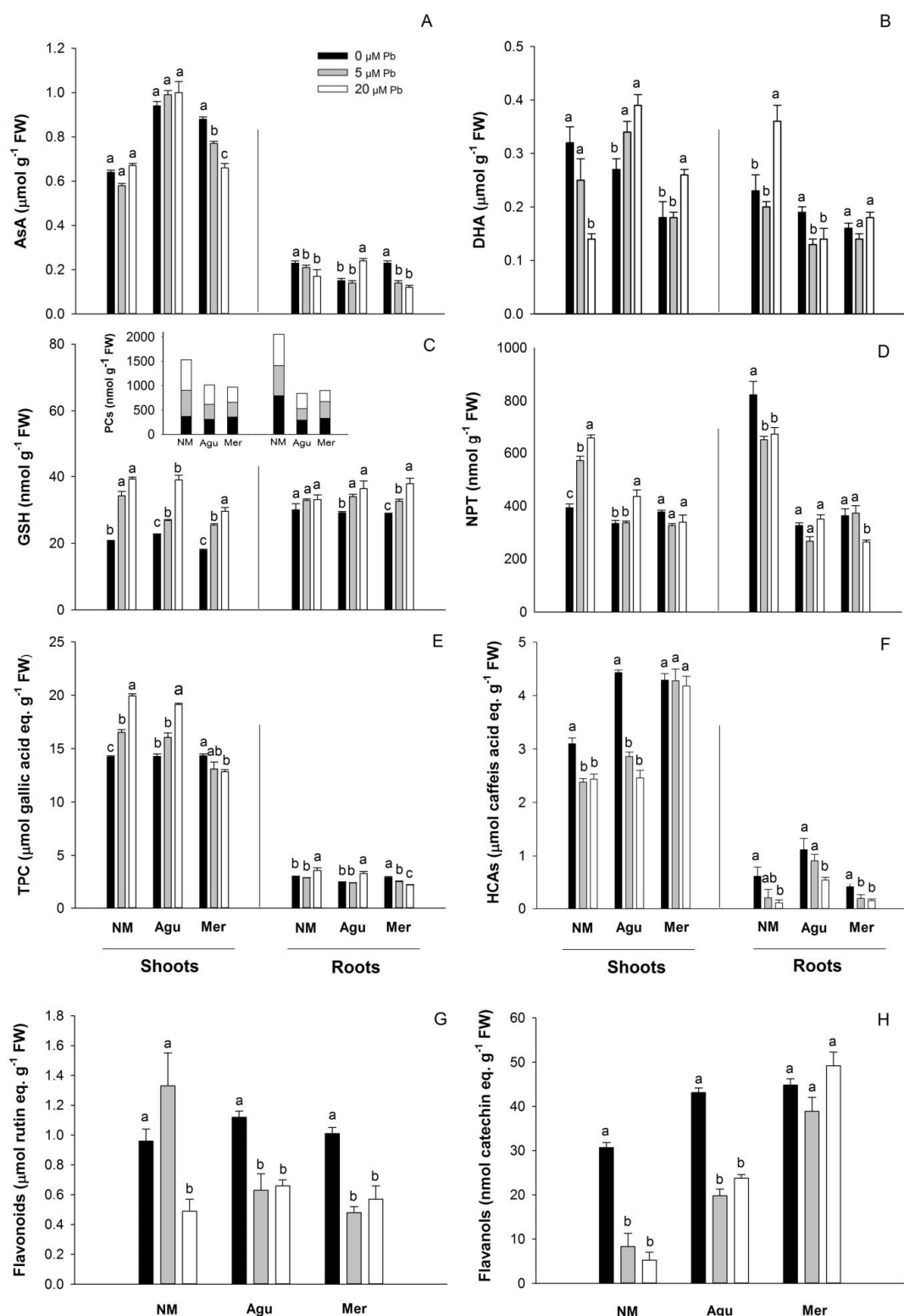


Figure 6. Redox profiles of the nonmetalliferous (NM) and metalliferous (M) populations of *Z. fabago* seedlings exposed for 4 weeks to low doses of Pb. Contents of AsA (ascorbate; (A)), DHA (dehydroascorbate; (B)), reduced glutathione (GSH) and phytochelatin (PCs; insert) (C), soluble total non-protein thiols (NPT; (D)), total soluble phenolics (TPC; (E)) and hydroxycinnamic acids (HCAs; (F)) in shoots, roots and flavonoids (G), as well as flavanols (H) contents in shoots of non-mining (NM) and mining Agustin (Agu) and Mercader (Mer) *Z. fabago* populations exposed to 0, 5 and 20 $\mu\text{M Pb}(\text{NO}_3)_2$ for 4 weeks. Values are given as mean \pm SE. Different letters correspond to significant differences between doses within the same population and organ ($p < 0.05$).

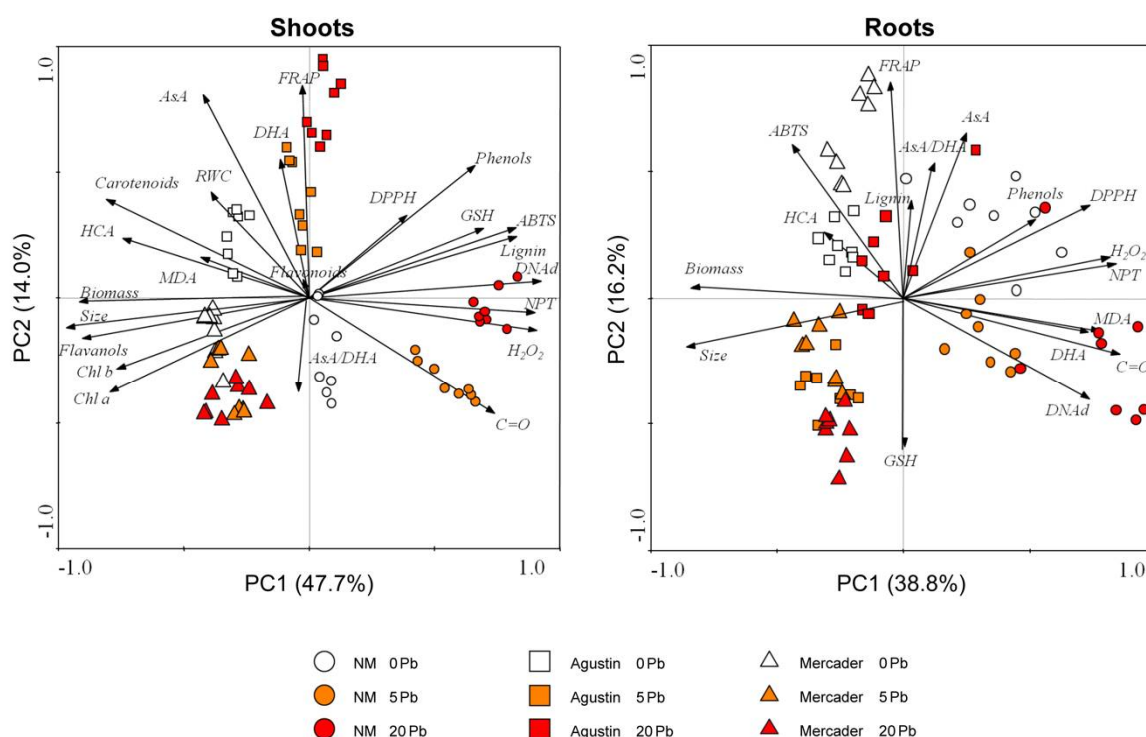


Figure 7. PCA analyses of functional responses of seedlings from non-mining (NM) and mining (Agustin and Mercader) *Z. fabago* populations exposed to 0, 5 and 20 μM $\text{Pb}(\text{NO}_3)_2$ for 4 weeks. For shoots, variance explained by the two first components was: X—axes 47.7% (PC1); Y—axes 14.0% (PC2). For roots, variance explained by the two first components was: X—axes 38.8% (PC1); Y—axes 16.2% (PC2).

4. Discussion

In this study, we used different biomarkers/endpoints of Pb cytogenotoxicity in order to understand the extent to which the seedlings from NM and M populations of the facultative, non-hyperaccumulator metallophyte *Z. fabago*, when exposed to chronic low Pb doses, mobilized lead from root to shoot and triggered defence mechanisms. Facultative metallophytes, such as *Z. fabago*, are described to tolerate metals which are in excess in their natural environments [32]. Here, there are evident differences in some phenotypic parameters between the mining and non-mining populations, even in the absence of Pb stress (control) (Table S1), which demonstrates the importance of the seed origin on the phenotype. Particularly interesting is the larger size (biomass and length), of both the shoots and roots, of the mining populations and higher contents of photosynthetic pigments which might contribute to the higher accumulation of Pb. The importance of phenotypes in this species has been discussed [13], and we suggest that, in this case, the phenotype of plants from mining areas is associated with a plant's capability to respond with a higher efficiency to metal accumulation as they develop higher adaptive mechanisms. Thus, seed/plant provenance, as well as the plant species, should be taken in consideration when selecting plants for phytoremediation programs.

4.1. Pb Uptake and Genotoxicity

In addition, the uptake and distribution of Pb in root and shoot tissues differed between the three populations studied. To prevent Pb entrance, plants have developed several barriers (e.g., the deposition of callose, formation of Fe/Mn plaques and binding to cell wall components) [33]. The intracellular protective mechanisms include Pb immobilization by chelation and sequestration in vacuoles [4]. In general, most of the Pb-tolerant species accumulated over 90% of the absorbed Pb in their roots and only a small amount was translocated to shoots [33]. Here, we observed that, although the non-mining population accumulated less Pb in their tissues, its translocation to shoots increased in a

dose-dependent manner. Conversely, despite the higher Pb concentrations in both the roots and shoots of M populations, their Pb transfer coefficients decreased with the increasing Pb dose in the substrate, particularly in Mercader seedlings. A higher Pb accumulation in above-ground organs in mining ecotypes, in comparison with non-mining ecotypes, was also described in different Pb-tolerant species such as *Silene vulgaris* [34] and *Bidens pilosa* [35]. Taken together, these results suggest differences in the regulatory mechanisms involved in Pb uptake, transport, and sequestration among the NM and M populations. Interestingly, despite the differences in the accumulation of Pb in roots and shoots, we observed the induction of DNA damage, evaluated by the comet assay, as well as the impairment of the cell cycle progression in all populations, even at doses of Pb as low as 5 μM . Nevertheless, the magnitude of DNA damage only showed a dose-dependent response in both the leaves and roots from the non-mining seedlings. Our data also revealed the particular susceptibility of NM seedlings to Pb-induced genotoxicity and its negative effect on growth regarding the negative correlation of DNA damage with size and biomass showed in the PCA analysis.

4.2. Cell Cycle Progression

The alteration in the cell cycle dynamics was observed in the leaves from NM and Mercader seedlings, whereas, in roots, Pb had cytostatic effects only in the Agustín population, with a decrease in the number of cells in peak II (the G_0/G_1 phase of subpopulation B + G_2 phase of subpopulation A). As diploid cells in the G_0/G_1 phase increased simultaneously with the detection of a decreasing trend in the number of cells in G_2 of the tetraploid population, it seems that Pb induces a delay and/or a blockage at the G_1/S check point in *Z. fabago*, particularly in diploid cells. The changes in cell cycle dynamics and/or ploidy levels in plants exposed to heavy metals were previously reported in lettuce plants exposed to Pb [18] and in pea roots exposed to Cr(VI) [36]. This trend of response may represent a cell strategy to cope with Pb-induced DNA damage, giving the cells extra time to repair DNA lesions [37]. It is worth mentioning that most karyotyped *Zygophyllum* populations were diploid and, more rarely, tetraploids [38]. For example, Amini-Chermahini et al. [39] reported Iranian populations of *Z. fabago* as diploids. However, it is important to highlight that the Zygophyllaceae *Larrea tridentata* can change from diploid to tetraploid and hexaploid, depending on the aridity of the environment [40]. Thus, to the best of our knowledge, this is the first report of the DNA-tetraploidy in *Z. fabago*, meaning that the putative variations in populations, and a genetic redundancy that contributes to the Pb tolerance properties of this pioneer species, remains unknown.

4.3. Oxidative Stress and Antioxidant Response

Pb is reported to induce an increase in intracellular ROS within plant cells, which could lead to a disruption of cellular redox homeostasis, against which an enzymatic and non-enzymatic antioxidant battery is triggered [4]. From our results, it is evident that the level of ROS (H_2O_2) accumulation, as well as the degree of biomolecules' oxidation/damage, was dependent on the plant's origin, being much higher in seedlings descended from the NM population. In this work we demonstrate that seedlings descending from non-mining populations trigger different antioxidant strategies compared to those from M populations, supporting previous findings of higher doses of Pb (25 and 50 μM) in the same *Z. fabago* populations [13].

Chloroplasts are major sources and targets of ROS, and thus contribute to the cellular redox balance [41]. Chlorophylls and carotenoids quantification may provide an insight into how plants maintain a fine balance between energy-linked functions and the control of ROS production. This balance was better evidenced in the seedlings descended from both M populations, suggesting that seedlings from seeds collected in mining sites are inherently better prepared to face induced photosynthetic impairments than seeds from uncontaminated sites. This was particularly evidenced by Mercader seedlings. Moreover, carotenoids also protect against ROS [42], and the reduction in their levels in NM seedlings

suggests a lesser capability to quench ROS, but also that the light-harvesting complex might be compromised by Pb.

Depending on the levels, H_2O_2 can act as a second messenger, regulating the gene expression of some antioxidant enzymes [43]. The distinct levels of this ROS in organs and populations exert different influences on specific antioxidant routes. Non-mining seedlings were unable to trigger an antioxidant response efficient enough to counteract the increase in ROS, impairing shoot growth (shown by the negative correlation between H_2O_2 and the growth parameters). Interestingly, the seedlings of the two M populations show variations in the antioxidant strategies, with Mercader seedlings responding more promptly to low Pb doses by up-regulating CAT gene expression [13], which suggests that these populations are already diverging in the defence strategies against Pb toxicity. On the other hand, the values of H_2O_2 and those from antioxidative tests from the roots of all populations were lower than the corresponding ones determined in shoots pointing to differentially expressed antioxidant responses in the organs.

To better understand the different models underlying the antioxidant responses in the roots and shoots of *Z. fabago* populations, the levels of the major components involved in the cellular redox state, GSH and AsA [41], as well as non-protein thiols (NPT) were analysed. Reduced GSH is known to work as an effective ROS scavenger and chelating bioligand for metals including Pb ions [44], and to trigger antioxidant pathways [45,46]. Here, GSH levels increased in the shoots of both NM and M populations, while in roots an increase was detected only in the M populations. These data are in agreement with the relevant role of GSH for coping with metal toxicity in plants [47]. Thus, the high Pb tolerance of M seedlings could be due, at least in part, to their capacity to increase the levels of GSH. Moreover, the lower levels of DNA damage found in M populations may be linked with higher contents of GSH, which also play a key role in controlling the redox balance of the nucleus [37]. GSH is also the precursor for the synthesis of phytochelatins (PCs), which bind and transport toxic metals to the vacuole to avoid their toxicity [4,47]. In our study, the chelation mechanism through NPT seems particularly significant in NM, in contrast to M, since the levels of PCs are constitutively higher in this population and, upon Pb exposure, the levels of PCs are upregulated in shoots. Although PCs are important chelators of Pb ions [4], it was suggested that the high energy costs associated with their biosynthesis seemed to make this Pb-detoxification strategy less cost-effective [48,49]. On the basis of our work, our results supported the idea that GSH, rather than PCs, are involved in the Pb detoxification in M populations, whereas in NM populations, PCs seem to play a more prominent role, this latter strategy being less effective at displaying a tolerance to Pb.

Plants have evolved different protective mechanisms in order to ensure survival and growth under adverse conditions. The synthesis and accumulation of phenolic compounds represent a well-known mechanism for stress amelioration in plants, including heavy metal exposure [50]. These compounds can protect plants against metal toxicity by metal chelation and direct ROS-scavenging capacities [50]. In fact, phenolic compounds such as HCAs and flavonoids, are known to be induced by metal exposure due to their antioxidant and metal-chelating properties [4,50,51]. In our study, the changes in the phenolic profile between seedlings derived from non-mining and mining populations may confer a higher Pb tolerance to the previous populations. On the other hand, phenolics, such as flavanols, whose levels are higher in Mercader, are able to scavenge ROS and detoxify H_2O_2 , acting as electron donors for peroxidases, which avoids or limits biomolecules oxidation [52]. The decrease in soluble phenolic compounds, especially in the “Mercader” population, may be explained by phenolics bonding to Pb or to their direct or indirect, peroxidase-mediated reaction with ROS, thus leading to a decrease in their quantification.

Interestingly, the apparently paradoxical reduction in AsA concentration in both the shoots and roots of Mercader seedlings, which is in line with previous results in the same species using higher Pb doses (25 and 50 μ M) [13], could be associated with the upregulation of extracellular, nonspecific peroxidases [53], which in turn could reduce H_2O_2 levels by using phenolics. The evidence of such a mechanism was recently reported

for a metallicolous population of *Z. fabago*, different from the population used in the present study, under controlled conditions [54], as well as for the same population used in this study in their natural environment [12]. In these studies, increases in peroxidase activities were correlated with both decreases in soluble phenolics and increases in cell wall-bound phenolics in the roots of plants challenged with Pb and in the shoots of plants naturally grown on metal-polluted soils, respectively.

In summary, the possible involvement of this phenolics/peroxidase system and other antioxidant enzymes [13], together with higher levels of phenolics, such as flavanols and HCAs, as well as thiol-based processes, may protect mining populations, especially Mercader, against high levels of biomolecules oxidation. In relation to this, it was reported that DNA fragmentation can be markedly reduced by monomeric and dimeric nuclear flavanols [52]. Hence, the lower levels of DNA damage found in M populations may be linked with higher contents of flavanols, further confirming that innate levels of antioxidative defence are pivotal in tolerating Pb stress.

5. Conclusions

In conclusion, we demonstrated that the chronic exposure to Pb doses lower than the maximum admissible for irrigation water in many countries, may induce cytogenotoxicity and cell cycle delay/blockage, as well as oxidative stress (lipid peroxidation and protein oxidation), particularly in non-mining *Z. fabago* populations. In contrast, the seedlings adapted to mining soils showed an increased absorption and tolerance to Pb toxicity. The higher innate levels of antioxidant compounds and the differential organ-specific response of redox metabolites seem to contribute to the tolerance to Pb exhibited by *Z. fabago* seedlings from mining sites. Thus, the maintenance of high GSH levels in both roots and shoots and high phenolics in shoots, mainly flavanols and HCAs, seems to be a low-cost strategy to counteract Pb toxicity in M seedlings. Overall, the results point out that the seed provenance may be relevant when phytostabilization and restoration programs of polluted soils are being developed, and these should be taken into consideration as they may increase the success of the programs.

Supplementary Materials: The following are available online at <https://www.mdpi.com/article/10.3390/horticulturae7110455/s1>, Table S1: Effect of Pb exposure on seed germination (%), shoot and root biomass and size, foliar RWC and photosynthetic pigments, and Pb accumulation seedling from non-mining (NM) and mining (Agustin and Mercader) *Z. fabago* populations exposed to 0, 5 and 20 μM $\text{Pb}(\text{NO}_3)_2$ for 4 weeks, Table S2: Percentage (%) of nuclei in each of the three identified peaks in leaves and roots of control and exposed plants: peak I— G_0/G_1 phase of the subpopulation A; peak II— G_0/G_1 phase of subpopulation B together with the G_2 phase of subpopulation A; peak III— G_2 phase of the subpopulation B, Table S3: Total antioxidant activity; AsA (ascorbate); DHA (dehydroascorbate); reduced glutathione (GSH) and soluble total non-protein thiols (NPT); total soluble phenolics (TPC); hydroxycinnamic acids (HCA); and flavonoids, flavanols, lignin, H_2O_2 , MDA and carbonyl (C=O) contents in shoots from non-mining (NM) and mining (Agustin and Mercader) *Z. fabago* populations exposed to 0, 5 and 20 μM $\text{Pb}(\text{NO}_3)_2$ for 4 weeks, Table S4: Total antioxidant activity, AsA (ascorbate); DHA (dehydroascorbate); reduced glutathione (GSH) and soluble total non-protein thiols (NPT); total soluble phenolics (TPC); hydroxycinnamic acids (HCA); and lignin, H_2O_2 , MDA, and carbonyl (C=O) contents in roots of nonmetalliferous (NM) and metalliferous (Agustin and Mercader) *Z. fabago* seedlings grown in the presence of increasing Pb concentrations (0, 5, and 20 μM) for 4 weeks.

Author Contributions: Conceptualization, C.S., M.Á.F. and A.A.C.; Formal analysis, A.L.-O., M.C.D. and S.S.; Funding acquisition, M.Á.F. and A.A.C.; Investigation, A.L.-O., M.C.D., H.O. and S.S.; Project administration, M.Á.F. and A.A.C.; Writing—original draft, A.L.-O., C.S., M.C.D. and S.S.; Writing—review and editing, C.S., M.C.D., H.O., M.Á.F., A.A.C. and S.S. All authors have read and agreed to the published version of the manuscript.

Funding: This work was funded by Fundação para a Ciência e Tecnologia (FCT) and Ministério da Educação e Ciência through national funds and the co-funding by the FEDER, within the PT2020 Partnership Agreement, and COMPETE 2010, within the projects of the CEF UI0183-UID/BIA/04004/2020, QOPNA research unit UID/QUI/00062/2019, LAQV-REQUIMTE UIDB/50006/2020 and CESAM (UIDP/50017/2020+UIDB/50017/2020). The FCT supported the research contracts of MC Dias (SFRH/BPD/100865/2014) and S Silva (SFRH/BPD/74299/2010) in the scope of the framework contract foreseen in the numbers 4, 5 and 6 of the article 23, of the Decree-Law 57/2016, of 29 August, changed by Law 57/2017, of 19 July and the research contract under the Stimulus of Scientific Employment 2017 H. Oliveira. (CEECIND/04050/2017). Thanks are due to the Spanish Government (CGL2006-11569 and CTM2011-23958) and Fundación Séneca (project FB/23/FS/ 02) for funding and for supporting A. López-Orenes FPU and mobility grants (AP2012-2559 and EST13/00414, respectively).

Institutional Review Board Statement: Not applicable.

Informed Consent Statement: Not applicable.

Data Availability Statement: To access these data, please contact the corresponding author.

Acknowledgments: The authors thank J. Dolezel (Institute of Experimental Botany, Olomouc, Czech Republic) for kindly providing *Pisum sativum* seeds.

Conflicts of Interest: The authors declare no conflict of interest.

References

- Mallhi, Z.I.; Rizwan, M.; Mansha, A.; Ali, Q.; Asim, S.; Ali, S.; Hussain, A.; Alrokayan, S.H.; Khan, H.A.; Alam, P.; et al. Citric acid enhances plant growth, photosynthesis, and phytoextraction of lead by alleviating the oxidative stress in castor beans. *Plants* **2019**, *8*, 525. [\[CrossRef\]](#)
- Egendorf, S.P.; Groffman, P.; Moore, G.; Cheng, Z. The limits of lead (Pb) phytoextraction and possibilities of phytostabilization in contaminated soil: A critical review. *Int. J. Phytoremed.* **2020**, *22*, 916–930. [\[CrossRef\]](#)
- Orroñoa, D.I.; Schindler, V.; Lavadoab, R.S. Heavy metal availability in *Pelargonium hortorum* rhizosphere: Interactions, uptake and plant accumulation. *J. Plant Nutr.* **2012**, *35*, 1374–1386. [\[CrossRef\]](#)
- Kumar, A.; Prasad, M.N.V. Plant-lead interactions: Transport, toxicity, tolerance, and detoxification mechanisms. *Ecotoxicol. Environ. Saf.* **2018**, *166*, 401–418. [\[CrossRef\]](#) [\[PubMed\]](#)
- Pourrut, B.; Shahid, M.; Dumat, C.; Winterton, P.; Pinelli, E. Lead Uptake, Toxicity, and Detoxification in Plants. *Rev. Environ. Contam. Toxicol.* **2011**, *213*, 113–136. [\[CrossRef\]](#)
- Rabęda, I.; Bilski, H.; Mellerowicz, E.J.; Napieralska, A.; Suski, S.; Woźny, A.; Krzesłowska, M. Colocalization of low-methylesterified pectins and Pb deposits in the apoplast of aspen roots exposed to lead. *Environ. Pollut.* **2015**, *205*, 315–326. [\[CrossRef\]](#) [\[PubMed\]](#)
- Sharma, S.S.; Dietz, K.-J. The relationship between metal toxicity and cellular redox imbalance. *Trends Plant Sci.* **2009**, *14*, 43–50. [\[CrossRef\]](#)
- Zine, H.; Midhat, L.; Hakkou, R.; El Adnani, M.; Ouhammou, A. Guidelines for a phytomanagement plan by the phytostabilization of mining wastes. *Sci. Afr.* **2020**, *10*, e00654. [\[CrossRef\]](#)
- Ernst, W.H.; Nelissen, H.J.; Bookum, W.M.T. Combination toxicology of metal-enriched soils: Physiological responses of a Zn- and Cd-resistant ecotype of *Silene vulgaris* on polymetallic soils. *Environ. Exp. Bot.* **2000**, *43*, 55–71. [\[CrossRef\]](#)
- Hego, E.; Vilain, S.; Barre, A.; Claverol, S.; Dupuy, J.-W.; Lalanne, C.; Bonneau, M.; Plomion, C.; Mench, M. Copper stress-induced changes in leaf soluble proteome of Cu-sensitive and tolerant *Agrostis capillaris* L. populations. *Proteomics* **2016**, *16*, 1386–1397. [\[CrossRef\]](#)
- Lefèvre, I.; Vogel-Mikuš, K.; Arčon, I.; Lutts, S. How do roots of the metal-resistant perennial bush *Zygophyllum fabago* cope with cadmium and zinc toxicities? *Plant Soil* **2016**, *404*, 193–207. [\[CrossRef\]](#)
- López-Orenes, A.; Bueso, M.C.; Conesa, H.M.; Calderón, A.; Ferrer, M.A. Seasonal changes in antioxidative/oxidative profile of mining and non-mining populations of *Syrian beancaper* as determined by soil conditions. *Sci. Total Environ.* **2017**, *575*, 437–447. [\[CrossRef\]](#)
- Ferrer, M.A.; Cimini, S.; López-Orenes, A.; Calderón, A.; De Gara, L. Differential Pb tolerance in metallicolous and non-metallicolous *Zygophyllum fabago* populations involves the strengthening of the antioxidative pathways. *Environ. Exp. Bot.* **2018**, *150*, 141–151. [\[CrossRef\]](#)
- López-Orenes, A.; Martínez-Pérez, A.; Calderón, A.A.; Ferrer, M.A. Pb-induced responses in *Zygophyllum fabago* plants are organ-dependent and modulated by salicylic acid. *Plant Physiol. Biochem.* **2014**, *84*, 57–66. [\[CrossRef\]](#) [\[PubMed\]](#)
- López-Orenes, A.; Dias, M.C.; Ferrer, M.A.; Calderón, A.; Moutinho-Pereira, J.; Correia, C.; Santos, C. Different mechanisms of the metalliferous *Zygophyllum fabago* shoots and roots to cope with Pb toxicity. *Environ. Sci. Pollut. Res.* **2018**, *25*, 1319–1330. [\[CrossRef\]](#) [\[PubMed\]](#)

16. Gichner, T.; Žnidar, I.; Száková, J. Evaluation of DNA damage and mutagenicity induced by lead in tobacco plants. *Mutat. Res. Toxicol. Environ. Mutagen.* **2008**, *652*, 186–190. [\[CrossRef\]](#)
17. Shahid, M.; Pinelli, E.; Pourrut, B.; Silvestre, J.; Dumat, C. Lead-induced genotoxicity to *Vicia faba* L. roots in relation with metal cell uptake and initial speciation. *Ecotoxicol. Environ. Saf.* **2011**, *74*, 78–84. [\[CrossRef\]](#)
18. Silva, S.; Silva, P.; Oliveira, H.; Gaivão, I.; Matos, M.; Pinto-Carnide, O.; Santos, C. Pb low doses induced genotoxicity in *Lactuca sativa* plants. *Plant Physiol. Biochem.* **2017**, *112*, 109–116. [\[CrossRef\]](#) [\[PubMed\]](#)
19. Zulfikar, U.; Farooq, M.; Hussain, S.; Maqsood, M.; Hussain, M.; Ishfaq, M.; Ahmad, M.; Anjum, M.Z. Lead toxicity in plants: Impacts and remediation. *J. Environ. Manag.* **2019**, *250*, 109557. [\[CrossRef\]](#)
20. Fischer, S.; Kühnlenz, T.; Thieme, M.; Schmidt, H.; Clemens, S. Analysis of plant Pb tolerance at realistic submicromolar concentrations demonstrates the role of phytochelatin synthesis for Pb detoxification. *Environ. Sci. Technol.* **2014**, *48*, 7552–7559. [\[CrossRef\]](#)
21. *Guidelines for Water Reuse 600/R-12/618*; Environmental Protection Agency (EPA): Washington, DC, USA, 2012.
22. Párraga-Aguado, I.; González-Alcaraz, M.; López-Orenes, A.; Ferrer-Ayala, M.; Conesa, H. Evaluation of the environmental plasticity in the xerohalophyte *Zygophyllum fabago* L. for the phytomanagement of mine tailings in semiarid areas. *Chemosphere* **2016**, *161*, 259–265. [\[CrossRef\]](#)
23. Gichner, T.; Patková, Z.; Száková, J.; Demnerová, K. Cadmium induces DNA damage in tobacco roots, but no DNA damage, somatic mutations or homologous recombination in tobacco leaves. *Mutat. Res./Genet. Toxicol. Environ. Mutagen.* **2004**, *559*, 49–57. [\[CrossRef\]](#)
24. Rodriguez, E.; Sousa, M.; Gomes, A.; Azevedo, R.; Mariz-Ponte, N.; Sario, S.; Mendes, R.J.; Santos, C. Genotoxic endpoints in a Pb-accumulating pea cultivar: Insights into Pb²⁺ contamination limits. *Environ. Sci. Pollut. Res.* **2019**, *26*, 32368–32373. [\[CrossRef\]](#) [\[PubMed\]](#)
25. Silva, S.; Santos, C.; Matos, M.; Pinto-Carnide, O. Al toxicity mechanism in tolerant and sensitive rye genotypes. *Environ. Exp. Bot.* **2012**, *75*, 89–97. [\[CrossRef\]](#)
26. Loureiro, J.; Rodriguez, E.; Dolezel, J.; Santos, C. Two new nuclear isolation buffers for plant dna flow cytometry: A Test with 37 Species. *Ann. Bot.* **2007**, *100*, 875–888. [\[CrossRef\]](#) [\[PubMed\]](#)
27. Pérez-Tortosa, V.; López-Orenes, A.; Martínez-Pérez, A.; Ferrer, M.A.; Calderón, A.A. Antioxidant activity and rosmarinic acid changes in salicylic acid-treated *Thymus membranaceus* shoots. *Food Chem.* **2012**, *130*, 362–369. [\[CrossRef\]](#)
28. López-Orenes, A.; Bueso, M.C.; Conesa, H.; Calderón, A.A.; Ferrer, M.A. Seasonal ionic and metabolic changes in *Aleppo pines* growing on mine tailings under Mediterranean semi-arid climate. *Sci. Total Environ.* **2018**, *637–638*, 625–635. [\[CrossRef\]](#)
29. Queval, G.; Noctor, G. A plate reader method for the measurement of NAD, NADP, glutathione, and ascorbate in tissue extracts: Application to redox profiling during *Arabidopsis* rosette development. *Anal. Biochem.* **2007**, *363*, 58–69. [\[CrossRef\]](#)
30. Hartley-Whitaker, J.; Ainsworth, G.; Vooijs, R.; Bookum, W.T.; Schat, H.; Meharg, A.A. Phytochelatin synthesis is involved in differential arsenate tolerance in *Holcus lanatus*. *Plant Physiol.* **2001**, *126*, 299–306. [\[CrossRef\]](#) [\[PubMed\]](#)
31. Hernández, J.A.; Ferrer, M.A.; Jiménez, A.; Barceló, A.R.; Sevilla, F. Antioxidant Systems and O₂⁻/H₂O₂ Production in the apoplast of pea leaves. Its relation with salt-induced necrotic lesions in Minor Veins. *Plant Physiol.* **2001**, *127*, 817–831. [\[CrossRef\]](#)
32. Ernst, W.H.O.; Verkleij, J.A.C.; Schat, H. Metal tolerance in plants. *Acta Bot. Neerl.* **1992**, *41*, 229–248. [\[CrossRef\]](#)
33. Efah, M.; Elaplaze, L.; Ebendaou, N.; Ehocher, V.; Mzibri, M.E.; Ebogusz, D.; Esmouni, A. Effect of lead on root growth. *Front. Plant Sci.* **2013**, *4*, 175. [\[CrossRef\]](#)
34. Mohtadi, A.; Ghaderian, S.M.; Schat, H. A comparison of lead accumulation and tolerance among heavy metal hyperaccumulating and non-hyperaccumulating metallophytes. *Plant Soil* **2012**, *352*, 267–276. [\[CrossRef\]](#)
35. Salazar, M.J.; Wannaz, E.D.; Blanco, A.; Pazcel, E.M.M.; Pignata, M.L. Pb tolerance and accumulation capabilities of *Bidens pilosa* L. growing in polluted soils depend on the history of exposure. *Chemosphere* **2021**, *269*, 128732. [\[CrossRef\]](#) [\[PubMed\]](#)
36. Rodriguez, E.; Azevedo, R.; Fernandes, P.; Santos, C. Cr(VI) induces dna damage, cell cycle arrest and polyploidization: A flow cytometric and comet assay study in *Pisum sativum*. *Chem. Res. Toxicol.* **2011**, *24*, 1040–1047. [\[CrossRef\]](#)
37. Cimini, S.; Gualtieri, C.; Macovei, A.; Balestrazzi, A.; De Gara, L.; Locato, V. Redox balance-DDR-miRNA triangle: Relevance in genome stability and stress responses in plants. *Front. Plant Sci.* **2019**, *10*, 989. [\[CrossRef\]](#)
38. Amini-Chermahini, F.; Ebrahimi, M.; Farajpour, M.; Bordbar, Z.T. Karyotype analysis and new chromosome number reports in *Zygophyllum* species. *Caryologia* **2014**, *67*, 321–324. [\[CrossRef\]](#)
39. Amini-Chermahini, F.; Ebrahimi, M.; Farajpour, M. Karyological studies in *Zygophyllum fabago* L. (Syrian bean caper) in Iran. *Caryologia* **2017**, *70*, 289–294. [\[CrossRef\]](#)
40. Laport, R.G.; Minckley, R.L.; Ramsey, J. Phylogeny and cytogeography of the north american creosote bush (*Larrea tridentata*, Zygophyllaceae). *Syst. Bot.* **2012**, *37*, 153–164. [\[CrossRef\]](#)
41. Foyer, C.H.; Noctor, G. redox regulation in photosynthetic organisms: Signaling, acclimation, and practical implications. *Antioxid. Redox Signal.* **2009**, *11*, 861–905. [\[CrossRef\]](#)
42. Niyogi, K.K. Safety valves for photosynthesis. *Curr. Opin. Plant Biol.* **2000**, *3*, 455–460. [\[CrossRef\]](#)
43. Chen, F.; Wang, F.; Wu, F.; Mao, W.; Zhang, G.; Zhou, M. Modulation of exogenous glutathione in antioxidant defense system against Cd stress in the two barley genotypes differing in Cd tolerance. *Plant Physiol. Biochem.* **2010**, *48*, 663–672. [\[CrossRef\]](#)
44. Kumar, G.H.; Kumari, J.P. Heavy metal lead influative toxicity and its assessment in phytoremediating plants—A Review. *Water Air Soil Pollut.* **2015**, *226*, 324. [\[CrossRef\]](#)

45. Sečenji, M.; Hideg, É.; Bebes, A.; Györgyey, J. Transcriptional differences in gene families of the ascorbate–glutathione cycle in wheat during mild water deficit. *Plant Cell Rep.* **2010**, *29*, 37–50. [[CrossRef](#)] [[PubMed](#)]
46. Jozefczak, M.; Remans, T.; Vangronsveld, J.; Cuypers, A. glutathione is a key player in metal-induced oxidative stress defenses. *Int. J. Mol. Sci.* **2012**, *13*, 3145–3175. [[CrossRef](#)]
47. Hernández, L.E.; Plata, J.S.; Montero-Palmero, M.B.; Carrasco-Gil, S.; Flores-Cáceres, M.L.; Ortega-Villasante, C.; Escobar, C. Contribution of glutathione to the control of cellular redox homeostasis under toxic metal and metalloid stress. *J. Exp. Bot.* **2015**, *66*, 2901–2911. [[CrossRef](#)] [[PubMed](#)]
48. Sun, Q.; Ye, Z.H.; Wang, X.R.; Wong, M.H. Increase of glutathione in mine population of *Sedum alfredii*: A Zn hyperaccumulator and Pb accumulator. *Phytochemistry* **2005**, *66*, 2549–2556. [[CrossRef](#)] [[PubMed](#)]
49. Gupta, D.; Huang, H.; Yang, X.; Razafindrabe, B.; Inouhe, M. The detoxification of lead in *Sedum alfredii* H. is not related to phytochelatins but the glutathione. *J. Hazard. Mater.* **2010**, *177*, 437–444. [[CrossRef](#)]
50. Michalak, A. Phenolic compounds and their antioxidant activity in plants growing under heavy metal stress. *Pol. J. Environ. Stud.* **2006**, *15*, 523–530.
51. Andjelkovic, M.; Vancamp, J.; Demeulenaer, B.; Depaemelaere, G.; Socaciu, C.; Verloo, M.; Verhe, R. Iron-chelation properties of phenolic acids bearing catechol and galloyl groups. *Food Chem.* **2006**, *98*, 23–31. [[CrossRef](#)]
52. Mouradov, A.; Spangenberg, G. Flavonoids: A metabolic network mediating plants adaptation to their real estate. *Front. Plant Sci.* **2014**, *5*, 620. [[CrossRef](#)] [[PubMed](#)]
53. Foyer, C.H.; Noctor, G. Redox homeostasis and antioxidant signaling: A metabolic interface between stress perception and physiological responses. *Plant Cell* **2005**, *17*, 1866–1875. [[CrossRef](#)] [[PubMed](#)]
54. López-Orenes, A.; Alba, J.M.; Kant, M.R.; Calderón, A.A.; Ferrer, M.A. OPDA and ABA accumulation in Pb-stressed *Zygophyllum fabago* can be primed by salicylic acid and coincides with organ-specific differences in accumulation of phenolics. *Plant Physiol. Biochem.* **2020**, *154*, 612–621. [[CrossRef](#)] [[PubMed](#)]